Sodium complexes containing 2-iminopyrrolyl ligands: The influence of steric hindrance in the formation of coordination polymers

ARTICLE *in* DALTON TRANSACTIONS · JANUARY 2010

Impact Factor: 4.2 · DOI: 10.1039/b905948b · Source: PubMed

7 AUTHORS, INCLUDING:

Clara S B Gomes
Technical University of Lisbon
44 PUBLICATIONS **201** CITATIONS
SEE PROFILE

Teresa Duarte
University of Lisbon
262 PUBLICATIONS **3,045** CITATIONS
SEE PROFILE

Teresa G. Nunes
Technical University of Lisbon
111 PUBLICATIONS **1,141** CITATIONS
SEE PROFILE

Maria Conceição Oliveira
Technical University of Lisbon
37 PUBLICATIONS **304** CITATIONS
SEE PROFILE

Sodium complexes containing 2-iminopyrrolyl ligands: the influence of steric hindrance in the formation of coordination polymers†

Clara S. B. Gomes, D. Suresh, Pedro T. Gomes,* Luis F. Veiros, M. Teresa Duarte, Teresa G. Nunes and M. Conceição Oliveira

Received 7th April 2009, Accepted 28th September 2009
First published as an Advance Article on the web 10th November 2009
DOI: 10.1039/b905948b

Iminopyrrolyl complexes of sodium were prepared from the reaction of 2-arylformiminopyrrole ligand precursors (aryl = C_6H_5 (**I**); 2,6-$Me_2C_6H_3$ (**II**); 2,4,6-$Me_3C_6H_2$ (**III**); 2,6-$^iPr_2C_6H_3$ (**IV**)) with one equivalent of sodium hydride. The resulting corresponding compounds **1–4**, $[\{Na(\mu_2{:}\kappa^2N,N'\text{-iminopyrrolyl})\}_{2n}(OEt_2)_{2x}]$ ($n \geq 1$; $x = 0$ or 1), were obtained in moderate to high yields and were characterised by NMR spectroscopy, high resolution mass spectrometry and X-ray diffraction, when suitable crystals were obtained. The X-ray structure of compound **1** ($n \gg 1$; $x = 0$) reveals the formation of a coordination polymer with repeating units consisting of dimers that contain two iminopyrrolyl ligands chelating two sodium atoms, where both pyrrolyl rings exhibit bridging σ + σ coordination to the Na atoms within the dimer; the self-assembling of the polymer is established by additional π-bonds (η^5-coordination) of each of the pyrrolyl rings to the sodium atoms of the adjacent dimer units. Conversely, the structure of complex $\mathbf{D^{IV}}$ ($n = x = 1$) shows it as one of such dimers capped by two diethyl ether molecules, each coordinated to the sodium atoms ($n = 2$; $x = 1$). DFT calculations indicate that the differences between the structures of **1–4** arise from the increasing bulkiness imposed by the corresponding substituents of the iminic aryl groups.

Introduction

Bidentate 2-iminopyrrole ligand precursors (Chart 1, **A**) are easily prepared by the condensation of 2-formylpyrrole with a variety of aliphatic or aromatic amines. In recent years, these compounds have attracted considerable attention in the areas of organometallic and coordination chemistry, and several classes of transition metal complexes containing bidentate iminopyrrolyl ligands (Chart 1, **B**) have been synthesised, being mainly used as polymerisation catalysts.[1,2] This interest has arisen from the high flexibility of their design, making possible the introduction of several kinds of steric and electronic features on the ligand, as required in polymerisation catalysis. Despite this current interest in the research and synthetic applications of iminopyrrolyl ligands, the first examples of homoleptic metal complexes of Co(II), Ni(II), Pd(II), Cu(II) and Zn(II) containing these kind of ligands, although only with alkylimino groups, were described in the 1960s.[3]

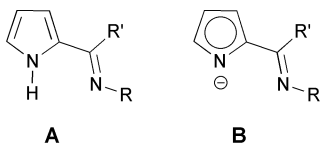

Chart 1 2-Iminopyrrole (**A**) and 2-iminopyrrolyl (**B**) derivatives.

Our group and other authors have been interested in the chemistry of arylamino derivatives of these ligands, having recently reported the synthesis and characterisation of several homoleptic complexes of Cr(II) and Cr(III),[4,5] Co(II),[6,7] Ni(II)[7,8,9] and Zn(II).[10,11] Group 4[7,12-18] and rare-earth[19,20] metal complexes containing iminopyrrolyl ligands have been particularly studied, in part due to their interest as olefin polymerisation catalysts.

The syntheses of these complexes are based on the deprotonation of iminopyrrole ligand precursors with a strong base, most usually Li^{n}Bu or NaH, and further reaction with the corresponding transition- or rare-earth metal salts. The intermediate alkali-metal iminopyrrolyl complexes are generally prepared and employed *in situ* and, for this reason, these species have rarely been isolated from solution[8,9] and poorly characterised in the solid state, particularly in what concerns their molecular structure. Conversely, despite the coordination of the simple pyrrolyl ligand to metals which has been extensively studied and its typical coordination modes characterised (Chart 2),[21] only a few examples involving this ligand and sodium are reported. Of particular significance to this work, and among other cases of pyrrolyl mixed π- and σ-coordination to sodium,[22,23] is the solid state structure of sodium 2,3,4,5-tetramethylpyrrolyl that was reported as polymeric, $[Na(NC_4Me_4)]_n$, the *catena*-(μ_3-η^5,σ^2-2,3,4,5-tetramethyl-1-sodiopyrrole-*N*,*N*), consisting of a double chain with alternating sodium and nitrogen atoms, in which each

Centro de Química Estrutural, Departamento de Engenharia Química e Biológica, Instituto Superior Técnico, Av. Rovisco Pais, 1049-001 Lisboa, Portugal. E-mail: pedro.t.gomes@ist.utl.pt; Fax: +351 218419612; Tel: +351 218419612

† Electronic supplementary information (ESI) available: Figures with representations of the asymmetric unit of ligand precursor **I** in polymorphic form **I_A**, NMR and high resolution mass spectra of compounds **1–4** and **4***, optimised DFT structures, and the corresponding tables of selected bond distances and angles, and atomic coordinates. CCDC reference numbers 727070–727074. For ESI and crystallographic data in CIF or other electronic format see DOI: 10.1039/b905948b

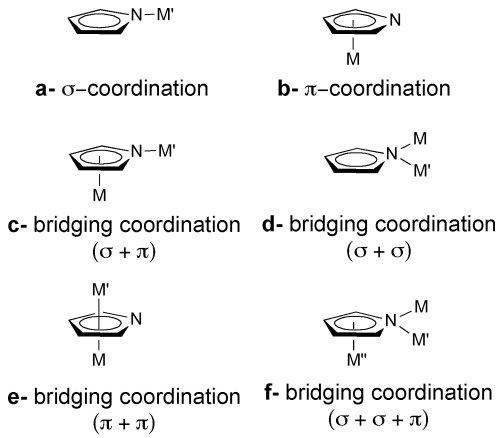

Chart 2 Types of coordination observed for pyrrolyl ligands.

pyrrolyl ligand is bridging (σ + σ + π) three sodium atoms (see form **f**, Chart 2).[21b,24,25]

Driven by the lack of structural information on sodium iminopyrrolyl compounds, and in light of our recent studies on transition-metal complexes containing 2-aryliminopyrrolyl ligands,[6,8] we decided to isolate and characterise a series of complexes of sodium in which these chelating ligands encompass an increasing bulkiness of the aryl substituent at the iminic nitrogen (C_6H_5; 2,6-$Me_2C_6H_3$; 2,4,6-$Me_3C_6H_2$ and 2,6-$^iPr_2C_6H_3$). These compounds were analysed by ^1H, ^{13}C and ^{23}Na NMR spectroscopy, high resolution laser desorption/ionisation mass spectrometry (HRMS) and, when possible, single-crystal X-ray diffraction. The use of DFT calculations[26] was made in order to help rationalise their solid state structures.

Results and discussion

Synthesis and characterisation of complexes

The four 2-arylformiminopyrrole ligand precursors (**I–IV**) used in this work (Scheme 1) were prepared by condensation of 2-formylpyrrole with several substituted arylamines, *i.e.* aniline, 2,6-dimethylaniline, mesitylaniline and 2,6-diisopropylaniline, employing standard conditions, according to the method described in previous publications by our group.[6,8] The corresponding formimines were obtained as solids or as crystals, with colours varying from pale yellow to orange-yellow and yields between 50 and 90%. The molecular structures of compounds **I** and **IV** were determined by single-crystal X-ray diffraction and are represented in Fig. 1. Selected bond distances and angles are listed in Table 1.

For both ligand precursors **I** and **IV**, the iminopyrrole fragment show planar backbones with similar structural features. Their structures also resemble those of other analogues.[6a,c,8] The most significant structural differences of these two compounds lie in the conformation of their aryl groups. In compound **IV**, the steric hindrance produced by the two bulky isopropyl substituents, at

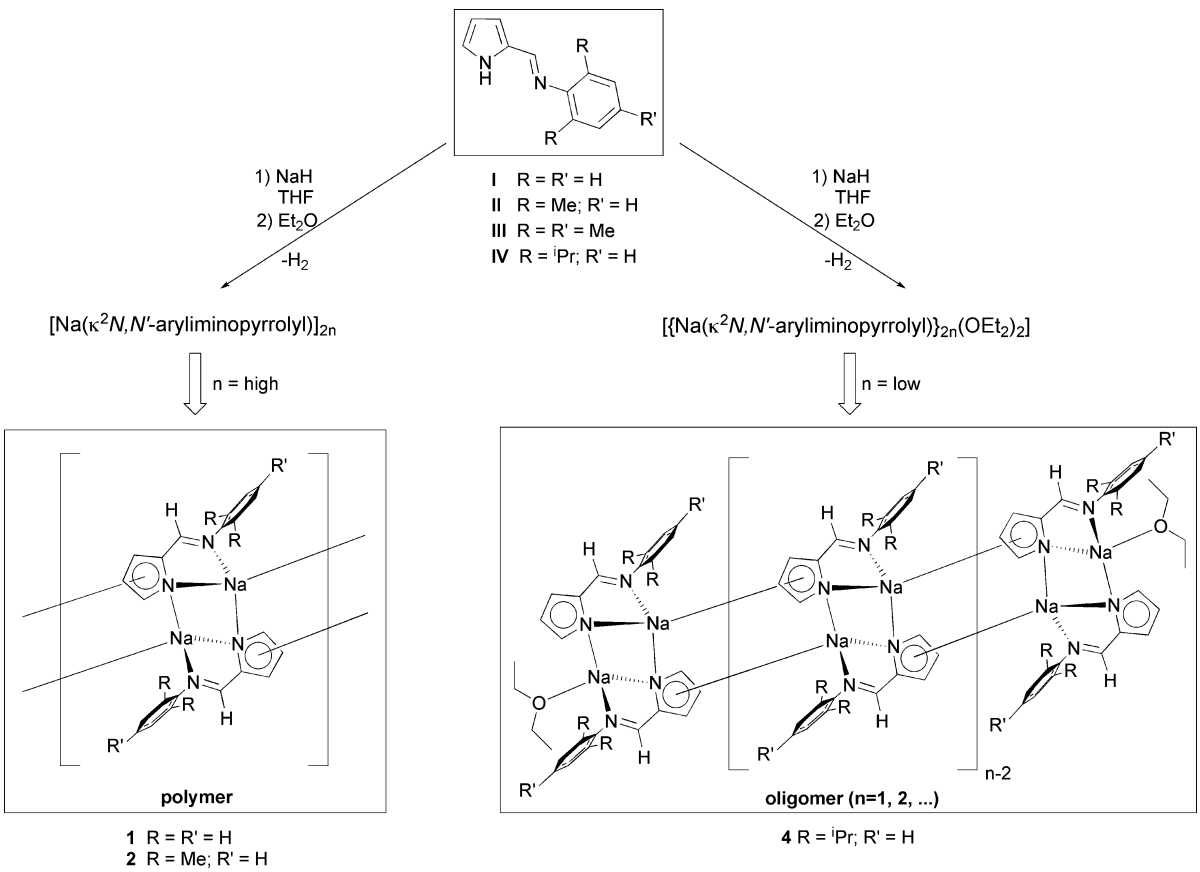

Scheme 1 Synthesis of sodium salts **1–4**.

Table 1 Selected bond distances (Å) and angles (°) for ligand precursors **I** and **IV**, and compounds **1** and $\mathbf{D^{IV}}$

	I		**IV**		**1**		$\mathbf{D^{IV}}$
Parameter	Molecule 1	Molecule 2	Molecule 1	Molecule 2	Ligand 1[a]	Ligand 2[a]	Ligand 1[b]
Distances							
N(1)–C(5)	1.3537(15)	—	1.357(2)	—	1.362(3)	—	1.354(4)
N(3)–C(16)	—	1.3596(17)	—	—	—	1.359(3)	—
N(3)–C(22)	—	—	—	1.353(2)	—	—	—
C(3)–C(4)	1.3974(18)	—	1.399(2)	—	1.381(3)	—	1.379(5)
C(14)–C(15)	—	1.3940(20)	—	—	—	1.386(3)	—
C(20)–C(21)	—	—	—	1.399(2)	—	—	—
C(6)–C(2)	1.4265(17)	1.4246(18)	1.431(2)	1.434(2)	1.427(3)	1.431(3)	1.424(4)
Na(1)–$\text{Pyrrolyl}_{\text{centroid}}$	—	—	—	—	2.447(3)	2.494(3)	—
Na(1)–O(1)	—	—	—	—	—	—	2.290(2)
Na(1)–N(1)	—	—	—	—	2.747(2)	—	2.405(3)
Na(1)–N(1_3)	—	—	—	—	—	—	2.404(3)
Na(1)–N(2)	—	—	—	—	—	—	2.428(3)
Na(2)–N(3)	—	—	—	—	—	2.676(2)	—
Na(1)–N(3)	—	—	—	—	—	2.404(2)	—
Na(1)–N(3_3)	—	—	—	—	—	2.439(2)	—
Na(1)–N(4)	—	—	—	—	2.436(2)	—	—
Na(2)–N(2_3)	—	—	—	—	—	2.691(2)	—
Na(2_3)–N(1)	—	—	—	—	2.524(2)	—	—
Na(2)–N(1_3)	—	—	—	—	2.398(2)	—	—
Na(1)–Na(1_3)	—	—	—	—	—	2.909(2)	2.956(3)
Na(2)–Na(2_3)	—	—	—	—	2.772(2)	—	—
Na(1)–Na(2_3)	—	—	—	—	—	2.633(2)	—
Angles							
N(3)–Na(1)–N(4)	—	—	—	—	—	96.43(7)	—
N(1)–Na(2)–N(2)	—	—	—	—	66.31(6)	—	—
N(1)–Na(1)–N(2)	—	—	—	—	—	—	72.45(11)

[a] In compound **1**, ligands 1 and 2 refer to the two crystallographically different iminopyrrolyl ligands binding both to Na(1) and Na(2) sodium atoms. Equivalent atoms are generated by the following symmetry operations: (1) $-x+2, -y+1, -z+2$; (2) $x, y-1, z$; (3) $-x+2, -y+2, -z+2$; (4) $x, y+1, z$. [b] In complex $\mathbf{D^{IV}}$, half of the molecule is generated by the symmetry operation $-x+1, -y, -z+1$.

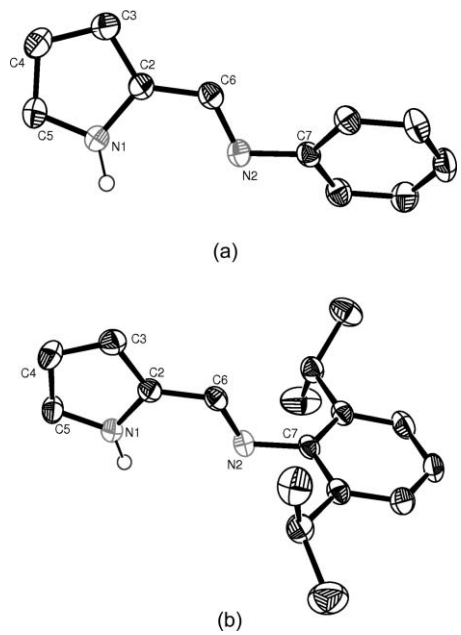

Fig. 1 ORTEP III diagram of the ligand precursors: (*a*) **I** and (*b*) **IV**, respectively, using 50% probability level ellipsoids. For both compounds, only one of the molecules of the asymmetric unit is represented. Calculated hydrogen atoms have been omitted for clarity.

positions 2 and 6 of the phenyl ring, makes it nearly perpendicular (dihedral angles of 84.21° and 87.34°, for molecule 1 and 2, respectively) to the formiminopyrrole plane defined by atoms N(2)–C(6)–C(2)–N(1). These values are very similar to those found for other substituted 2-aryliminopyrrole derivatives.[6a,c,8] Conversely, in compound **I**, the phenyl fragment lies approximately half way between perpendicular and coplanar to the formiminopyrrole plane (dihedral angles of 47.03° and 41.08° for molecules 1 and 2, respectively), due to a much less hindered rotation about the N(2)–C(7) bond. In fact, this is even more evident in the crystal structure of a polymorphic form of **I**, crystallised from toluene, compound **I_A** (monoclinic system and $P2_1/c$ space group),[27] where one of the four molecules of phenyliminopyrrole of the asymmetric unit exhibits a phenyl ring almost coplanar with the iminopyrrole fragment (dihedral angle of 8.90°). All the crystalline structures of the ligand precursors **I**, **I_A** and **IV** show self-assembly of two formiminopyrrole molecules, by the formation of two complementary H bonds (NH ⋯ N distances varying between 2.01(2) and 2.25(2) Å) between a pyrrole NH and an imine nitrogen belonging to the other molecule of the pair, in agreement with the findings reported in the literature.[6c,28]

Treatment of ligand precursors **I–IV** with one equivalent of sodium hydride in THF at −20 °C, resulted in the deprotonation of the pyrrole NH proton, giving rise to the formation of the formiminopyrrolyl sodium salts **1–4** (Scheme 1). Workup of the reaction mixtures in diethyl ether, and subsequent crystallisation/precipitation, gave rise to beige crystals of **1**, off-white powders of **2** and **3**, and a pale pink microcrystalline powder of **4**, in moderate to high yields (53–82%) (Scheme 1). All these materials are very sensitive to air and moisture.

The structure of compound **1** was determined by X-ray diffraction, showing a solid state structure in which the smallest fragments [Na(κ²*N*,*N*′-phenylformiminopyrrolyl)] are dimerised with sodium bridges, the dimers being enchained through Na–pyrrolyl π-bonding to form a ladder-type coordination polymer.

Compound **1** exhibits a polymeric structure (Fig. 2, Table 1), which is somehow related to that described for the sodium 2,3,4,5-tetramethylpyrrolyl,[24] and also for sodium[29a] and potassium pyrazolyl.[29b] It can be regarded as a chain of dimer repeating units, related by a symmetry centre, in which two identical iminopyrrolyl ligands are chelating two identical sodium atoms and, simultaneously, both pyrrolyl rings exhibit bridging σ + σ coordination (see Chart 2, **d**) to both sodium atoms (Fig. 2(*a*)). The formation of the polymer chain is due to the self-assembling of repeating dimer units. This occurs through the establishment of additional π-bonds, by η⁵-coordination of each of the pyrrolyl rings and sodium atoms of a particular dimer to the complementary counterparts in the adjacent dimer units. In the present case, two crystallographically different dimers alternate in the chain, the iminopyrrolyls of each are chelating the corresponding sodium atoms with bite angles of 66.3 (N(1)–Na(2)–N(2)) and 71.9° (N(3)–Na(1)–N(4)). In each of these alternating dimers, the phenyl groups are parallel to each other, but exhibit different conformations, being approximately either perpendicular (Na1 dimers) or parallel (Na2 dimers) to the polymer chain direction, with a dihedral angle of 76° between their ring planes. As shown in Fig. 2(*b*), this supramolecular arrangement seems to be dictated by the existence of two aromatic CH/π hydrogen bonds[30] (C–H8 $\cdots$ $Ph_{centroid}$ = 2.870 and C–H11 $\cdots$ $Ph_{centroid}$ = 2.976 Å) between the phenyl groups of adjacent dimers, which may additionally contribute to the polymeric enchainment. Compound **1** is therefore a fine example of an alkali-amide ladder polymer,[25] and can be alternatively described as an enchainment of repeating units [Na(κ²*N*,*N*′-iminopyrrolyl)], which are bound to each other in such a way that two chains of alternating sodium and nitrogen atoms combine the characteristic features of amide bridges with η⁵-coordination of pyrrolyl rings (Fig. 2(*b*)). The imino "arms" appear alternating in a syndiotactic-like arrangement in relation to the ladder backbone. Within the polymer, each of the pyrrolyl nitrogens is thus involved in a bridging σ + σ + π coordination (see Chart 2, **f**). The geometry around each sodium atom is that of a distorted three-legged piano stool, which may be considered as eight-coordinate, as a result of the η⁵-coordination of the pyrrolyl ring. The Na–Na distance in the Na1 dimer repeating units (2.909(2) Å) is higher than that observed for Na2 dimers (2.772(2) Å), with a distance of 3.633 Å between Na1 and Na2 atoms. As observed for sodium 2,3,4,5-tetramethylpyrrolyl[24] and for lithium carbazolide,[31] the two single bonds Na–N(pyrrole) at each sodium atom have different lengths and the Na–N bond involved in η⁵-bonding is also longer for both cases.

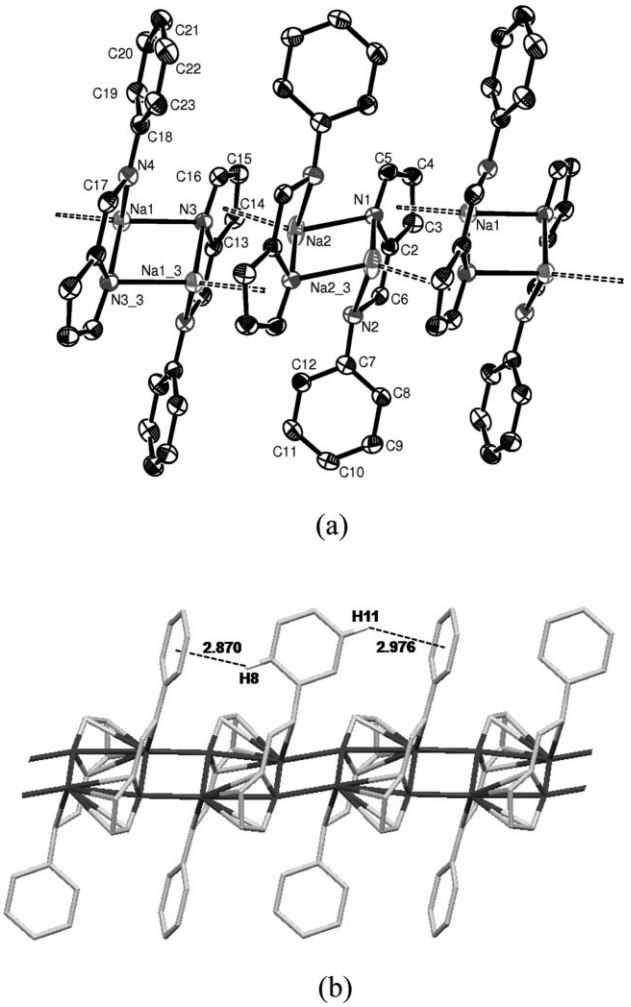

Fig. 2 (*a*) ORTEP III diagram of a segment of three consecutive [Na(κ²*N*,*N*′-iminopyrrolyl)]₂ repeating dimer units in the molecular structure of polymeric **1**. The dashed lines represent the η⁵-coordination of pyrrolyl rings (centroids) to the sodium atoms. (*b*) Mercury diagram of the polymeric ladder backbone made of alternating nitrogen and sodium atoms, exhibiting a syndiotactic-like arrangement of the phenylimino groups, and aromatic CH/π hydrogen bonds between adjacent phenyl groups. For both diagrams, hydrogen atoms have been omitted for clarity.

On the other hand, we managed to isolate single-crystals from the bulk of a sample of the sodium salt **4**, and determined the X-ray structure of the dimeric compound [Na(μ₂:κ²*N*,*N*′-2,6-diisopropylphenylformiminopyrrolyl)(OEt₂)]₂ **D**^{IV} (labelled by the letter "**D**" with a superscript indicating the ligand precursor), whose structure is represented in Chart 3 and Fig. 3. The dimer **D**^{IV} corresponds to the particular case where $n = 1$ in the general structure of the oligomeric compound **4**, depicted in Scheme 1. In the crystal structure of **D**^{IV}, half the molecule of the dimer is

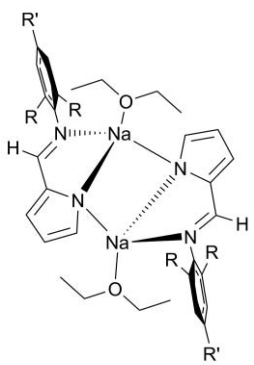

D^{IV} R = ^{i}Pr; R' = H

Chart 3 Structure of dimer **D**^{IV}.

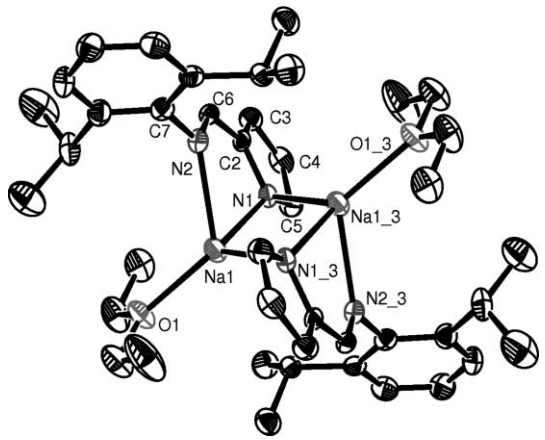

Fig. 3 ORTEP III diagram of complex $\mathbf{D^{IV}}$, using 50% probability level ellipsoids. Half molecule is generated by the symmetry operation $1 - x, -y, 1 - z$. Hydrogen atoms have been omitted for clarity.

generated by the symmetry operation $1 - x$, $-y$, $1 - z$. In this bimetallic sodium complex, each of the iminopyrrolyl ligands is chelating a different sodium atom with a bite angle N(1)–Na(1)–N(2) of 72.45° and, simultaneously, both pyrrolyl rings exhibit bridging $\sigma + \sigma$ coordination (see Chart 2, **d**) to both sodium atoms. The latter sodium atoms are somewhat more distant (2.956(3) Å) than those in the corresponding dimer repeating units of polymer **1** (2.772(2) and 2.909(2) Å), and show tetrahedral geometries. This structure, although very different, is reminiscent of the dimeric nature of the repeating unit of polymer **1**. It suggests that the much bulkier character of the 2,6-diisopropyl aryl substituents hinders the formation of π-bonding of the pyrrolyl rings and aryl CH/π bonding, therefore hampering the self-assembling of these dimers into oligomers or polymers, due to high steric congestion. Instead, a diethyl ether solvent molecule occupies the fourth coordination position of sodium atoms, giving rise to the bimetallic sodium dimer $\mathbf{D^{IV}}$.

It should be remarked that, upon coordination, the structural features of the iminopyrrolyl ligands in compounds **1** and $\mathbf{D^{IV}}$ only show minor changes in relation to their parent neutral molecules **I** and **IV**.

The solubility behaviour of compounds **1–4** is a key issue for their structural interpretation. Salt **1** is virtually insoluble in aliphatic and aromatic hydrocarbons, sparingly soluble in CH_2Cl_2, moderately soluble in the weakly-coordinating Et_2O, and very soluble in strongly-coordinating solvents such as THF or CH_3CN. The solubilities of compounds **2** and **3** are similar to those of **1**, although somehow more soluble in CH_2Cl_2. Conversely, salt **4** is partially soluble in aromatic hydrocarbons, and very soluble in CH_2Cl_2, Et_2O, THF and CH_3CN. This solubility behaviour, along with the observed ^1H, ^{13}C and ^{23}Na NMR features in solution, indicates that the polymeric or oligomeric solid state structures are essentially broken upon dissolution by the coordinative nature of the solvent, due to disruption of the weaker Na–pyrrolyl π-bonding. This will give rise to soluble species with a much lower degree of association, presumably dimeric or even monomeric complexes containing solvent adducts, respectively, $[Na(\mu_2{:}\kappa^2N,N'\text{-aryliminopyrrolyl})L]_2$ or $[Na(\kappa^2N,N'\text{-aryliminopyrrolyl})L_2]$ (L= coordinating solvent, *e.g.* CD_3CN, THF), where only the σ bonds between the Na ions and the chelating ligand persist. These observations agree with those of Kuhn *et al*. for the sodium 2,3,4,5-tetramethylpyrrolyl.[24] The behaviour observed in solution for compounds **2** and **3**, being very similar to that of **1**, strongly suggests that these are polymeric materials too, since they are also practically insoluble in non-coordinating organic solvents.

The HRMS spectra (see ESI†) show, for all compounds, parent ion peaks corresponding to the isotopic distribution expected for $[Na(iminopyrrolyl)]^+$ species, with a 1 : 1 metal : ligand stoichiometry, identical to that employed in the synthetic procedure. No solvent adduct species were detected, probably due to their dissociation in the gas phase. Electron-spray ionisation mass spectra were not conclusive since they revealed only the presence of the parent ion peaks of the protonated ligand precursors **I–IV**.

NMR studies

All compounds were characterised by ^1H, ^{13}C and ^{23}Na NMR, in acetonitrile-d_3 (see Experimental and ESI†). The ^1H and ^{13}C NMR spectra of compounds **1–3** showed only resonances belonging to an iminopyrrolyl moiety. However, in the ^1H NMR spectrum of salt **4**, besides the iminopyrrolyl resonances, it was also possible to observe a quartet and a triplet corresponding, respectively, to the methylene (CH_2) and methyl (CH_3) protons of a diethyl ether molecule. We also found that the molar ratio Et_2O/iminopyrrolyl is not easily reproduced in the double-layering recrystallisations (with Et_2O and n-hexane), and is extremely sensitive to the precipitation conditions. In fact, for compound **4**, we obtained molar ratios Et_2O/iminopyrrolyl as different as 0.82 and 0.38, using Et_2O solutions either close to saturation, in the latter case, or more diluted conditions, in the first case. For a pure sample of dimer $\mathbf{D^{IV}}$, one should expect a theoretical molar ratio Et_2O/iminopyrrolyl of 1 and, therefore, a value of 0.82 means the sample is composed by a majority of dimer $\mathbf{D^{IV}}$, but it also contains other oligomers with $n > 1$ (tetramer, hexamer, *etc.*; see Scheme 1). These oligomers are capped with two Et_2O molecules, each of them coordinating the sodium atoms of both terminal end groups of the oligomer. In fact, the single-crystal of $\mathbf{D^{IV}}$ was obtained in a sample of **4** with a molar ratio Et_2O/iminopyrrolyl of 0.82 ($[Na(\mu_2{:}\kappa^2N,N'\text{-}2,6\text{-}^i Pr_2Ph\text{-formiminopyrrolyl})(OEt_2)_{0.82}]$). Conversely, a sample with a molar ratio of 0.38 ($[Na(\mu_2{:}\kappa^2N,N'\text{-}2,6\text{-}^i Pr_2Ph\text{-formiminopyrrolyl})(OEt_2)_{0.38}]$) is close to an average n value of 3, which corresponds approximately to a hexamer as an average molecule (theoretical value of 0.33, *i.e.* $1/n$). These types of ladder-oligomeric structures with capping solvent molecules have already been observed in lithium amides and phosphides.[25]

However, salts **4** are relatively unstable to vacuum atmosphere since the Et_2O molecules are weakly coordinated to the sodium ions. In fact, there is a clear decrease in the ether content of **4** that depends on the number of vacuum/dinitrogen cycles applied to the compound and on their corresponding times and pressures. This can be monitored by ^1H NMR and can result in the complete loss of the ether molecules from the material. We have labelled the samples of **4** that have completely lost their Et_2O molecules when subjected to vacuum, as **4***.

The ^1H chemical shifts observed for the iminopyrrolyl ligands of compounds **1–4** and **4*** are only slightly different when compared with those observed for the free molecules (either the iminopyrrole ligand precursor **I–IV** or the Et_2O). The ^{23}Na NMR spectra

Table 2 Solution and solid state ^{23}Na NMR data of complexes **1–4** and **4***: chemical shifts and half-height width of complexes in CD_3CN solution; number of species, relative concentration and nuclear parameters obtained by fitting of the ^{23}Na MAS NMR spectra, the fitting factors being related to the spectral residues

	Solution[a]		Solid state					
Compound	δ (ppm)	$\Delta\nu_{1/2}$/Hz	Number of species	Relative concentration [b](%)	δ_{iso} (ppm)	C_q/MHz	η	Fitting factor (%)
1	4.056	353	2	99	−5.71 ± 0.13	4.53 ± 0.04	0.42 ± 0.05	7.5
				1	−19.92 ± 0.73	0.00	0.00	
2	4.305	428	1	100	4.62 ± 0.47	3.91 ± 0.16	0.59 ± 0.09	7.1
3	4.394	529	2	95.5	8.91 ± 0.5	3.47 ± 0.20	0.77 ± 0.06	18.9[c]
				4.5	−14.04 ± 0.68	0.00	0.00	
4	4.233	400	2	57	15.27 ± 0.71	3.59 ± 0.13	0.78 ± 0.10	11.7
				43	−8.30 ± 0.82	5.75 ± 0.06	0.99 ± 0.01	
4*[d]	4.591	550	2	75	11.47 ± 0.24	4.32 ± 0.03	0.75 ± 0.02	11.4
				25	−18.72 ± 0.37	5.23 ± 0.26	0.33 ± 0.16	

[a] Solvent: CD_3CN. [b] Only the central transition was used in the calculation. [c] The spectral S/N ratio is low due to experimental constraints making impossible to obtain a better fitting factor. [d] Sample where the Et_2O molecules have been removed by vacuum.

of complexes **1–4** and **4***, obtained in CD_3CN, showed single resonances with almost invariant chemical shifts in the range δ 4.06 to 4.59 ppm and with half-height widths ($\Delta\nu_{1/2}$) varying between 353 and 550 Hz (see Table 2 and the corresponding spectra in the ESI†), typical of the quadrupolar ^{23}Na nucleus,[32] meaning that, in these solutions, the species are structurally very similar.

^{23}Na magic angle spinning (MAS) solid state NMR spectra were also acquired from compounds **1–4** and from a sample of **4***. The central transition frequency of the ^{23}Na spectrum (a quadrupolar nucleus of spin 3/2) depends on the orientation of each crystallite in the static magnetic field, to second order in perturbation theory. The electric field gradient (EFG) at the nucleus depends on the geometry of bonds around it and arises from any lack of symmetry in the local electron distribution; the asymmetry parameter η is a measure of axial symmetry of the EFG tensor ($0 \leq \eta \leq 1$ and $\eta = 0$ for an axially symmetric EFG). The quadrupolar coupling constant, $C_q = e^2qQ/h$, represents the quadrupolar interaction between the nuclear electric quadrupole moment (eQ, where e is the proton charge), which is constant for a given nuclear species, and the EFG at the nucleus (eq). A relationship should be expected between C_q, the ligand–Na distance and the local symmetry about the sodium atom; spherical symmetry was shown to produce unimportant EFG, that is, small C_q.[33] Two contributions determine the ^{23}Na isotropic chemical shift (δ_{iso}): diamagnetic (high field shift effect) and paramagnetic shielding (downfield shift effect). While with MAS technique the dipolar and first order quadrupolar broadening can be reduced and in some cases zeroed, the second order quadrupolar broadening is maintained.

Different sodium species could be identified in compounds **1–4** and **4*** by analyzing their specific δ_{iso}, C_q and η, which are presented in Table 2. Fig. 4 shows all the spectra, represented along with their simulations (also see superimpositions of experimental and simulated spectra in Fig. S6, S11, S16, S24 and S29, ESI†), from which the relative concentration and quadrupolar parameters of Na species were obtained (Table 2). A general trend in ^{23}Na chemical shifts has been established as a result of numerous studies:[34] ^{23}Na δ_{iso} decreases with increasing coordination number (CN) and increasing Na-donor atom distance but it is necessary to differentiate contributions from different functional groups.

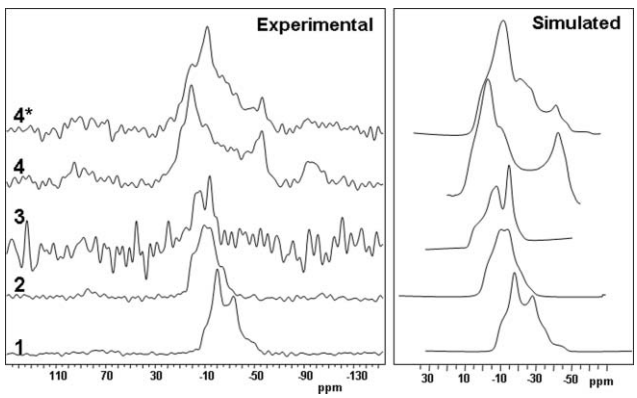

Fig. 4 ^{23}Na MAS NMR (experimental and simulated) spectra obtained for compounds **1–4** and **4***.

Table 2 shows that δ_{iso} of the most abundant species, which are the inner sodium nuclei with a CN of 8, increases with the volume of aryliminopyrrolyl substituent groups: δ_{iso} −5.71 ± 0.13, 4.62 ± 0.47 and 8.91 ± 0.5 ppm were obtained for compounds **1** to **3**. Moreover, C_q decreases from compounds **1** to **3** by about 1 MHz; these species do not present EFG tensors with axial symmetry (η is 0.42 ± 0.05 and 0.77 ± 0.06, for compounds **1** and **3**, respectively). To rationalise δ_{iso} and C_q variations, it may be concluded that the average N_{imino}–Na and $N_{pyrrolyl}$–Na distance decreases from samples **1** to **3**, in which case lower symmetry at the sodium atom could explain the high C_q value; δ_{iso} appears to be more sensitive than C_q to the structural effects being investigated. On the other hand, signals at high magnetic field in **1** and **3** spectra (δ_{iso} −19.92 ± 0.73 and −14.04 ± 0.68 ppm) are tentatively assigned to the chain terminal Na atoms, in spite of an envisaged lower CN.

As far as complexes **4** and **4*** are concerned, two sodium species were identified in each compound, with relative concentrations of *ca.* 3/2 and 3/1, respectively (Table 2); δ_{iso} were 15.27 ± 0.71 and 11.47 ± 0.24 ppm, for the species observed at low magnetic field, which also do not present EFG tensors with axial symmetry (the corresponding C_q were 3.59 ± 0.13 and 4.32 ± 0.03 MHz). By comparison with compounds **1** to **3**, the average N_{imino}–Na and $N_{pyrrolyl}$–Na distances appears to decrease in complexes **4** and **4*** (shorter average distance in **4**). Actually, a comparison between the

Na–N distances, within the dimer units of polymer **1** (see Table 1), show longer distances than those observed in dimer $\mathbf{D^{IV}}$. Similar to compounds **1** and **3**, signals at high magnetic field (δ_{iso} −8.30 ± 0.82 and −18.72 ± 0.37 ppm) are tentatively assigned to the terminal Na atoms, which bind the Et_2O capping molecules in **4**.

The comparison of **1** to **4** tetramer structures using DFT calculations (see DFT studies) indicate that their major differences lie in the conformations of the aryl rings and that, for the terminal sodium species, the Na–O distances are in the range 2.33–2.36 Å. The Na–Na distances inside the dimer units are similar in **1** and **4** tetramers, but the central Na–Na separation, between dimers connected by Na–pyrrolyl π-bonding, is slightly shorter in the case of **1** than in **4**; the geometric features of tetramers **2** and **3** are intermediate between those of **1** and **4**, which agree well with the trend obtained for δ_{iso} (Table 2). A similar downfield shift tendency was reported in the ^{23}Na NMR studies of sodium cyclopentadienyl (NaCp, $\delta_{iso} = -57.5$ ppm) and its tetrahydrofuran solvate CpNa·THF ($\delta_{iso} = -45.5$ ppm);[35] at room temperature, it was observed that C_q increased with increasing substitution of the Cp ring, but a full molecular orbital analysis of the origin of chemical shielding in polymeric sodocenes was not performed in order to explain the unusually high shielding of sodium nuclei.[36]

Table 2 also shows that the chemical shifts measured in CD_3CN for compounds **1** to **3** follow a trend similar to solid state data. However, as already highlighted, the solid state structures of compounds **1** to **3** are not retained in solution; overall, in CD_3CN, similar structures have to be assigned to all compounds thus reflecting the similarity of the corresponding ^{23}Na chemical shifts. In liquids, the sodium line width depends both on quadrupolar interaction and correlation time, which characterises the EFG fluctuation.[37] Hence, under comparable correlation time, the increase of the line width from complexes **1** to **3** (353 to 529 Hz) reflects a quadrupolar interaction increase, which is consistent with an increase in conformational stability; conversely, similar C_q data would imply different correlation time in order to explain the line width tendency. Further ^{23}Na NMR studies are beyond the scope of the present investigation.

The presence of a second type of Na atom in very low concentrations (1 and 4.5%, respectively) in the polymeric materials **1** and **3** may be attributed to the chain end groups (Scheme 1). It is likely that the apparent absence of terminal sodium atoms in compound **2** is related to the high molecular weight of the polymer, meaning that the terminal sodium content is beyond the detection limit of this method. In the polymer formation, it is expected that Et_2O molecules cap the chain ends by coordination to the terminal sodium atoms. However, these Et_2O ligands are labile due to their weak bonding nature to sodium, being easily removed from their sites by the simple application of vacuum in the workup and/or manipulation of the compounds (Scheme 2, route a). The ^{23}Na MAS NMR spectrum of compound **4** with a molar ratio Et_2O/iminopyrrolyl = 0.38 (Fig. 4) reveals a high content of terminal groups (inner Na/terminal Na = 3/2, not very far from the theoretical value of 2/1 for a hexamer), since two well defined species are present in the spectrum. However, for a sample of **4***, in which the Et_2O molecules have been removed by vacuum evaporation, the presence of the same two species of Na atoms of **4** is clearly seen, but now with a lower concentration of terminal groups (inner Na/terminal Na = 3/1). A process could be envisaged in which the Et_2O removal would induce the assembling of some of the unsaturated dimers or oligomers in the solid state, giving rise to higher molecular weight oligomers (Scheme 2, route b). In the present case, the ratio of internal to terminal sodium atoms is 3/1, which corresponds to an average polymerisation degree of 4 dimers (eight sodium atoms, *i.e.* octamers), if one considers that both terminal Na atoms are equivalent and represented by the minor upfield ^{23}Na

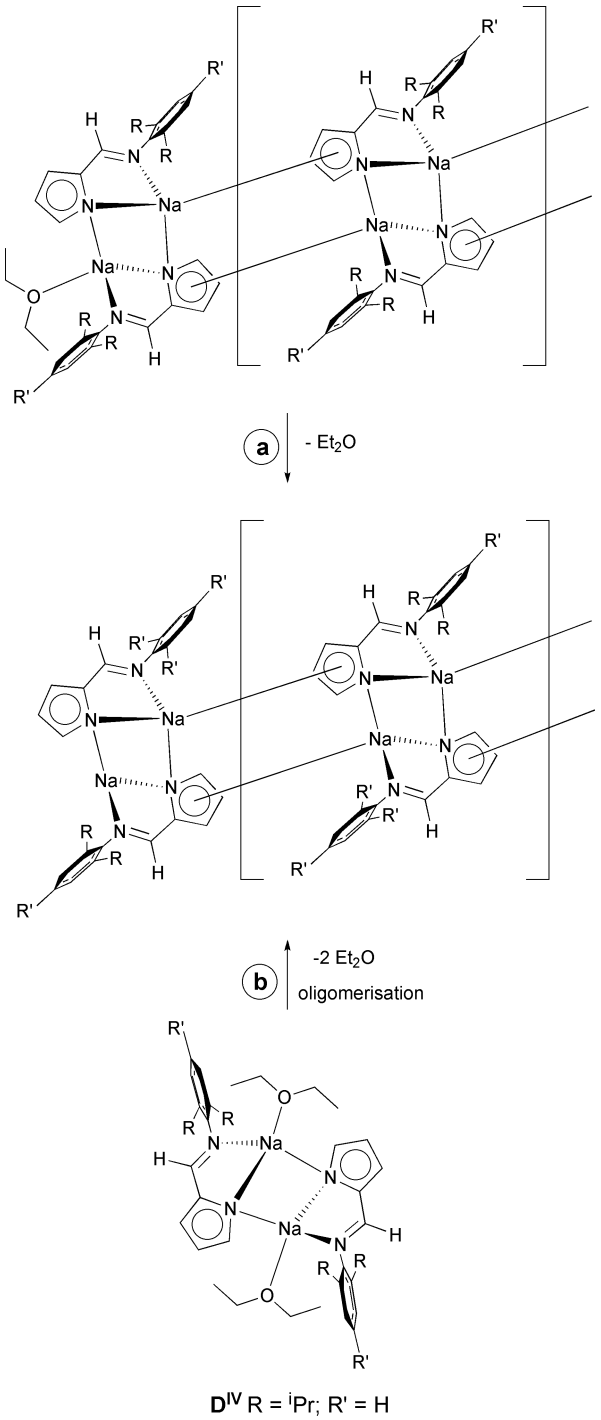

Scheme 2 Types of terminal groups of compounds **1–4** and **4***, and possible formation of oligomers from $\mathbf{D^{IV}}$ by vacuum removal of Et_2O molecules.

resonance. Using the same rationale, we could estimate degrees of polymerisation of 100 and 22 dimers for **1** and **3**, respectively.

DFT studies

The structural preferences of sodium complexes **1–4** were addressed by means of DFT calculations.[26] Dimeric structures, such as that determined experimentally for complex $\mathbf{D^{IV}}$ (see above), were optimised for all the iminopyrrolyl ligands derived from precursors **I–IV**. The structure calculated for the unsubstituted phenyliminopyrrolyl ligand derived from the ligand precursor **I** (R = R′ = H) is represented in Fig. 5. Figures representing all optimised species are presented in the ESI† (see Fig. S30).

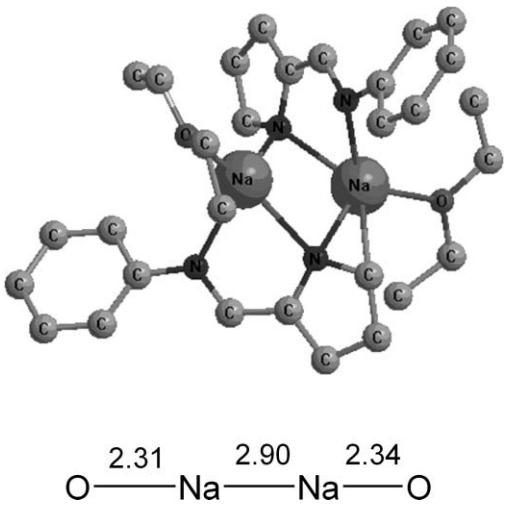

Fig. 5 Optimised structure (PBE1PBE/6-31G**) obtained for the dimeric complex [Na(μ_2:κ²*N*,*N*′-phenylformiminopyrrolyl)(OEt_2)]$_2$ ($\mathbf{D^I}$) derived from ligand precursor **I**. The Na–Na and Na–O distances (Å) are indicated and the H-atoms are omitted for clarity.

All optimised dimers closely resemble the X-ray structure of complex $\mathbf{D^{IV}}$, discussed above. In fact, the structure calculated for $\mathbf{D^{IV}}$ can be used as a test to the performance of the computational method employed. The maximum (Δ) and mean (δ) absolute deviations between the calculated and the experimental bond distances involving the Na-atoms were Δ = 0.08 Å and δ = 0.03 Å, and, in addition, a value of 82° is calculated for the dihedral angle between the plane of the aryl and the plane of the iminopyrroyl moiety, corresponding to a perfect match with the experimental value. These values demonstrate that the theoretical method used provides a good description of the systems, at least from a structural point of view. This conclusion is important given the significant ionic character expected in the species studied.

A closer observation of the structures calculated for all dimers (labelled by the letter "**D**" with a superscript indicating the ligand precursor) confirms the similarity of all the species $\mathbf{D^I}$–$\mathbf{D^{IV}}$ (Scheme 3). The difference between the various complexes lies in the aryl substituents of the aryliminopyrrolyl ligand, R = R′ = H for $\mathbf{D^I}$, R = Me and R′ = H in the case of $\mathbf{D^{II}}$, R = R′ = Me for $\mathbf{D^{III}}$ and, finally, R = ^{i}Pr and R′ = H in the case of $\mathbf{D^{IV}}$. In all cases there is a σ + σ coordination mode of the pyrrolyl rings and the dimer geometry is capped by two diethyl ether molecules, coordinated each to a Na-atom. The relevant distances are similar in all dimers. The Na–O separations vary from 2.31 Å, in $\mathbf{D^I}$, to 2.35 Å in the remaining three species, and the Na–Na bond length is slightly shorter in $\mathbf{D^I}$ (2.90 Å), than in the salts with iminopyrrolyl ligand having 2,6- or 2,4,6-substituted aryl rings (d_{Na-Na} = 3.04 Å for $\mathbf{D^{II}}$–$\mathbf{D^{IV}}$). The dihedral angles between the aryl plane and the plane of the iminopyrrolyl moiety in the dimers provide an additional mean for comparison between the complexes. The values obtained for $\mathbf{D^I}$ are 33° for one of the ligands, and 34° for the other, while in the case of the dimers with substituted ligands the aryl rings are practically perpendicular with respect to the iminopyrroyl plane (the corresponding angles being 87, 85 and 82° for $\mathbf{D^{II}}$, $\mathbf{D^{III}}$ and $\mathbf{D^{IV}}$, respectively). Interestingly, these angles reproduce the trend observed in the X-ray structures of ligand precursors **I** and **IV** discussed above.

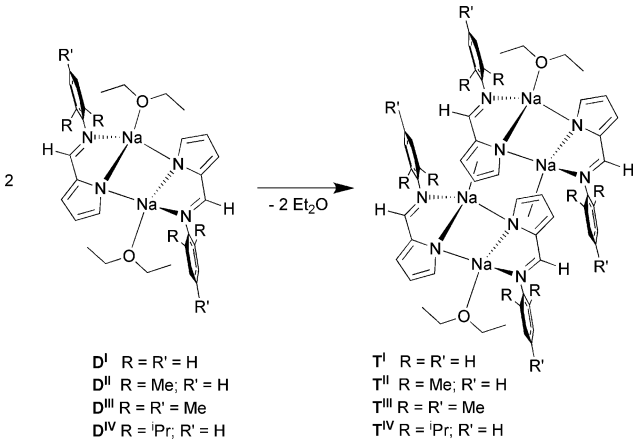

Scheme 3 The formation of a tetramer from the condensation reaction of two dimers.

The tendency of the iminopyrrolyl sodium salts to form polymeric structures was probed through DFT geometry optimisations performed on tetramers comprising four [Na(iminopyrroyl)] units. Those species correspond to the assembling of two dimers, with consequent loss of two diethyl ether molecules, one in each of the original dimers (Scheme 3). In the final structure, the two dimer units are bonded together through the establishment of π-coordination involving pyrrolyl rings and Na-atoms on adjacent dimers. Two of such interactions exist in each tetramer, involving complementary parts of the dimers. Thus, the two central pyrrolyl rings will adopt a σ + σ + π coordination mode similarly to what is observed in the polymeric structure of **1**. In fact, the formation of the tetramers, represented in Scheme 3, can be viewed as the first step of a condensation process of the dimers towards the formation of a polymer.

Along this discussion, the tetramers will be labelled by the letter "**T**" with a superscript indicating the ligand precursor (see Scheme 3). Thus, $\mathbf{T^{IV}}$, will correspond to the tetramer of the type [{Na(iminopyrrolyl)}$_4$(OEt_2)$_2$] in which the ligand is originated from precursor **IV** (R = ^{i}Pr and R′ = H). The geometry calculated for $\mathbf{T^I}$ and $\mathbf{T^{IV}}$ are represented in Fig. 6. Figures with the optimised geometry of all tetramers are presented as supplementary information (Fig. S31, ESI†).

In the general structure calculated for the tetramers there are two types of pyrrolyl rings. The two outer pyrrolyl rings present σ + σ coordination connecting the two Na-atoms inside each dimer moiety by means of *N*-bridges. Conversely, the two internal pyrrolyl rings adopt σ + σ + π coordination, holding the

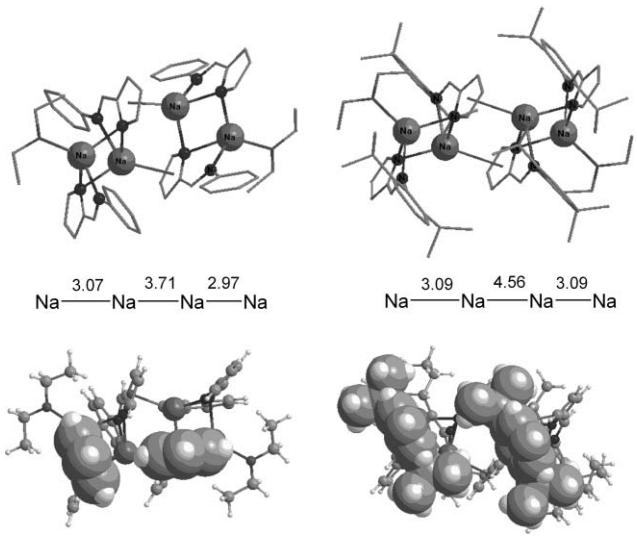

Fig. 6 Optimised structures (PBE1PBE/6-31G**) of the tetramers $\mathbf{T^{I}}$ (left) and $\mathbf{T^{IV}}$ (right). Top: general view with the Na- and *N*-atoms highlighted. The H-atoms are omitted for clarity, and the Na–Na distances (Å) are shown. Bottom: side view emphasising the relative conformation of the aryl rings.

two dimers together through π-coordination between Na-atoms and ligands on adjacent dimer units. Interestingly, the general geometric features of $\mathbf{T^{I}}$ are closely related to those presented by polymer **1**. The Na–Na separations inside each dimer unit in $\mathbf{T^{I}}$ (2.97 and 3.07 Å) are significantly shorter that the distance between Na-atoms belonging to opposite dimers (3.71 Å). The previous distances, calculated for tetramer $\mathbf{T^{I}}$, are within 0.08–0.20 Å of the equivalent ones in the X-ray structure of **1**. Moreover, the relative conformation of the phenyl rings with respect to the rest of the iminopyrrolyl frame is also similar in the calculated tetramer and in **1**, as shown by the dihedral angle between the corresponding planes: 38–50° in $\mathbf{T^{I}}$, compared to 36 and 47° in the X-ray structure of **1**.

Comparing all the tetramer structures, the Na–O distances are in the range 2.33–2.36 Å, being similar to those observed in the X-ray structure of $\mathbf{D^{IV}}$ (2.29 Å). The conformation of the aryl rings is one of the major differences between the structures of the two tetramers represented in Fig. 6. In the species with substituted 2,6-aryl groups ($\mathbf{T^{IV}}$), these rings are almost perpendicular with respect to the iminopyrrolyl framework (the corresponding dihedral angles, calculated for $\mathbf{T^{IV}}$, are 69–70°), contrarily to the intermediate conformation presented by $\mathbf{T^{I}}$ (see above). The presence of the 2,6-^{i}Pr substituents, in $\mathbf{T^{IV}}$, determines the conformation of the aryl rings in each iminopyrrolyl ligand, and, as a consequence, dictates the relative arrangement of the two consecutive aryl groups in the structure, *i.e.*, the two 2,6-aryl substituents on the same side of the tetramer. As shown in the bottom of Fig. 6, in $\mathbf{T^{IV}}$ the two consecutive aryl rings are almost parallel, with dihedral angles between aryl planes of 11°, while for the tetramer with plain phenyl rings ($\mathbf{T^{I}}$), the two consecutive rings present an almost perpendicular arrangement, with dihedral angles of 65 and 72°, between the planes of each pair of consecutive phenyl rings (one on each side of the tetramer). In addition, as a consequence of the stereochemical repulsion, the aryl rings are farther apart in the case of $\mathbf{T^{IV}}$ than in $\mathbf{T^{I}}$, as demonstrated by the distances between the C_6-ring centroids for each pair of aryl groups: 7.15 and 7.16 Å for $\mathbf{T^{IV}}$, and 5.34 and 5.63 Å for $\mathbf{T^{I}}$. This means that in the structure of $\mathbf{T^{IV}}$ the two dimer units are more distant than in the case of $\mathbf{T^{I}}$, or, in other words, the enhanced steric bulk of the aryl substituents, in $\mathbf{T^{IV}}$, pushes away the two dimer units in the tetramer, making the corresponding structure closer to two separated dimers. This effect is clearly shown by the Na–Na distances in the tetramers. The Na–Na distances inside dimer units are similar for the two tetramers (2.97 and 3.07 Å for $\mathbf{T^{I}}$, and 3.09 Å for $\mathbf{T^{IV}}$), but the central Na–Na separation is significantly shorter in the case of $\mathbf{T^{I}}$ (3.71 Å) than in $\mathbf{T^{IV}}$ (4.56 Å). The geometric features of tetramers $\mathbf{T^{II}}$ and $\mathbf{T^{III}}$ are intermediate between those of $\mathbf{T^{I}}$ and $\mathbf{T^{IV}}$ discussed above.

The energy balance calculated for the reaction of tetramer formation, from the corresponding pair of dimers, that is, the reaction represented in Scheme 3, can be used to probe the tendency to form polymer structures for each Na(iminopyrrolyl) salt. A small positive value was obtained for the formation of $\mathbf{T^{I}}$ from two dimers $\mathbf{D^{I}}$ ($\Delta E = 1.7$ kcal mol^{-1}), while in the case of the ligand with 2,6-^{i}Pr$_2$C$_6$H$_3$ aryl groups, *i.e.*, for the formation of $\mathbf{T^{IV}}$ from two dimers $\mathbf{D^{IV}}$, the energy balance is considerably less favourable ($\Delta E = 10.3$ kcal mol^{-1}). This shows the enhanced stereochemical repulsion existing in structures with higher degree of assembling, when bulky substituents are present in the aryl groups of the iminopyrrolyl ligands, being in agreement with the above X-ray data, *i.e.*, the observation of a polymeric structure for salt **1**, and of isolated dimers for $\mathbf{D^{IV}}$. The energy balance calculated for the formation of the other two tetramers ($\mathbf{T^{II}}$ and $\mathbf{T^{III}}$) presents a value ($\Delta E = 6.6$ kcal mol^{-1}) intermediate between the two discussed above, indicating that, when the ligand has methyl substituents in the aryl ring (ligand precursors **II** and **III**), the corresponding sodium salt will have a tendency to polymerise that should be intermediate between that verified for **1** and for $\mathbf{D^{IV}}$. Nevertheless, the solubility experimental data, namely the requirement of a coordinating solvent, seem to indicate that those salts adopt a polymer structure similar to that determined for **1**.

Conclusions

A series of iminopyrrolyl compounds of sodium were prepared from the reaction of 2-arylformiminopyrrole ligand precursors (aryl = C_6H_5 (**I**); 2,6-$Me_2C_6H_3$ (**II**); 2,4,6-$Me_3C_6H_2$ (**III**); 2,6-$^{i}Pr_2C_6H_3$ (**IV**)) with one equivalent of sodium hydride. The resulting corresponding compounds **1–4**, [{Na(μ$_2$:κ^2*N*,*N*′-iminopyrrolyl)}$_{2n}$(OEt$_2$)$_{2x}$] ($n \geq 1$; $x = 0$ or 1) were obtained in moderate to high yields, their solid state structures varying from oligomers ($n = 2, 3, \ldots; x = 1$), in the case of complex **4**, to polymers ($n \gg 2$; $x = 0$), in the case of **1–3**. The coordination polymer chains consist of dimers similar to those found for complex $\mathbf{D^{IV}}$ ($n = x = 1$), in which the diethyl ether capping molecules were replaced by other similar dimers. The chain formation results from the self-assembling of unsaturated dimer repeating units through the establishment of additional π-bonds (η^5-coordination) of each of the pyrrolyl rings to the sodium atoms of the adjacent dimer units. DFT calculations indicate that the differences between the structures of **1–4** arise from the increasing bulkiness imposed by the substituents of the iminic aryl groups.

Experimental

General considerations

All experiments dealing with air- and/or moisture-sensitive materials were carried out under inert atmosphere using a dual vacuum/nitrogen line and standard Schlenk techniques. Nitrogen gas was supplied in cylinders by specialized companies (*e.g.* Air Liquide, *etc*) and purified by passage through 4 Å molecular sieves. Unless otherwise stated, all reagents were purchased from commercial suppliers (*e.g.* Acrös, Aldrich, Fluka) and used without further purification. All solvents to be used under inert atmosphere were thoroughly deoxygenated and dehydrated before use. They were dried and purified by refluxing over a suitable drying agent followed by distillation under nitrogen. The following drying agents were used: sodium (for diethyl ether and tetrahydrofuran) and calcium hydride (for n-hexane). Deuterated solvents were dried by storage over 4 Å molecular sieves and degassed by the freeze–pump–thaw method. Solvents and solutions were transferred using a positive pressure of nitrogen through a stainless steel cannula and mixtures were filtered in a similar way using a modified cannula that could be fitted with glass fibre filter disks.

Nuclear magnetic resonance (NMR) spectra in solution were recorded on a Bruker 300 MHz spectrometer at the following frequencies: ^{1}H at 300.130 MHz; ^{13}C at 75.4753 MHz or on a Bruker 400 MHz spectrometer at the following frequencies: ^{1}H at 400.132 MHz; ^{13}C at 100.623 MHz and ^{23}Na at 105.842 MHz. The spectra were referenced internally using the residual protio solvent resonance relative to tetramethylsilane ($\delta = 0$), for ^{1}H and ^{13}C spectra, and externally relative to NaCl 1M in aqueous solution, for ^{23}Na spectra. The latter spectra were obtained after digital subtraction of the ^{23}Na resonance characteristic of the 5 mm tube glass material, which was measured in a blank experiment performed with an empty tube. All chemical shifts are quoted in δ (ppm) and coupling constants given in Hz. Multiplicities were abbreviated as follows: broad (br), singlet (*s*), doublet (*d*), triplet (*t*), quartet (*q*), heptet (*h*) and multiplet (*m*). For air- and/or moisture-stable compounds, samples were dissolved in $CDCl_3$ and prepared in common NMR tubes. The NMR assignments of the pyrrole ring were made according to the X-ray labelling. The molar ratios Et_2O/iminopyrrolyl were determined using the normalised Et_2O and iminopyrrolyl resonances of the ^{1}H NMR spectra, which were acquired with relaxation delays of 60 s, in order to obtain accurate integrations. For air- and/or moisture-sensitive materials, samples were prepared in J. Young tubes, using a glovebox. ^{23}Na NMR solid state spectra were acquired following a single RF pulse excitation (Bloch decay) on a Bruker MSL 300P spectrometer, using 4 mm *o.d.* zirconia rotors, at 79.365 MHz; a pulse duration of 1.0 μs (flip angle of *ca.* 10°) was used at a spinning speed of about 7.6 kHz. All the chemical shifts are referenced to aqueous NaCl ($\delta = 0$). To obtain the NMR parameters of each sodium species, the spectra were simulated using the program QUASAR.[38]

The high resolution laser desorption/ionisation mass spectra were obtained on a Finnigan FT/MS 2001-DT equipped with a 3 Tesla superconductor and interfaced with a Nd:YAG laser operating at the fundamental wavelength 1064 nm.

The compound 2-formylpyrrole was prepared according to a literature procedure.[39] The synthesis of the ligand precursors **I–IV** was made according to a procedure already used in previous publications.[6,8] This general procedure was adapted from the literature for **I**[14,40] and **IV**.[7,41,42]

Synthesis of sodium salts (1–4)

The same procedure presented in previous publications was followed.[6,8] In a typical experiment, NaH (24 mg, 1.0 mmol) was suspended in tetrahydrofuran and 1.0 mmol of a neutral ligand precursor (**I–IV**), at –20 °C, was slowly added as a solid under a counter flow of nitrogen. An immediate evolution of hydrogen occurred, and after some minutes, a solution of the sodium ligand salt was obtained. The cold bath was removed and the solution was allowed to warm to room temperature, and then stirred for 90 min. All volatiles were evaporated and the resulting residue was washed with n-hexane and extracted with diethyl ether until extracts were colourless or the entire residue was extracted. The solution was partially concentrated under vacuum (*ca.* 50%), double-layered with n-hexane (1 : 3) and stored at –20 °C, yielding 0.16 g (82%) of beige crystals of **1**, 0.18 g (80%) of an off-white solid of **2**, 0.13 g (56%) of an off-white solid of **3** or 0.17 g (53%) of pale pink crystals of **4**, respectively. Compound **4**, which contains Et_2O in its composition, is not stable in vacuum atmosphere, losing its Et_2O content after long periods under vacuum or several cycles vacuum/nitrogen, giving rise to the fully desolvated material **4***.

Data for 1. HRMS Found: *m/z* 193.03929 $[M + H]^+$. Calc. For $[C_{11}H_{10}N_2Na]^+$: 193.07417. NMR [δ_H (300 MHz, CD_3CN)]: 8.17 (1H, s, N=CH), 7.31–7.27 (2H, m, aryl *o*-H), 7.17–7.15 (2H, m, aryl *m*-H), 7.04–6.99 (2H, m, pyrrole H4 and aryl *p*-H), 6.58 (1H, dd, $^{4}J_{HH} = 1.2$ Hz and $^{3}J_{HH} = 3.2$ Hz, pyrrole H5), 6.09 (1H, dd, $^{4}J_{HH} = 1.2$ Hz and $^{3}J_{HH} = 3.3$ Hz, pyrrole H3). NMR [δ_H (400 MHz, CD_2Cl_2)]: 8.27 (1H, br s, N=CH), 7.37 (2H, br s, aryl *o*-H), 7.17 (3H, br s, aryl *m*- and *p*-H), 7.01 (1H, br s, pyrrole H4), 6.67 (1H, br s, pyrrole H5), 6.31 (1H, br s, pyrrole H3). NMR [δ_C (75 MHz, CD_3CN)]: 156.3 (N=CH), 155.1 (aryl *ipso*-C), 140.1 (pyrrole C2), 137.4 (aryl *p*-C), 129.8 (aryl *m*-C), 123.8 (pyrrole C5), 121.9 (aryl *o*-C), 120.4 (pyrrole C3), 110.6 (pyrrole C4). NMR [δ_{Na} (105 MHz, CD_3CN)]: 4.06 (s, $\Delta\nu_{1/2} = 353$ Hz).

Data for 2. HRMS Found: *m/z* 221.10818 $[M + H]^+$. Calc. For $[C_{13}H_{14}N_2Na]^+$: 221.10547. NMR [δ_H (400 MHz, CD_3CN)]: 7.69 (1H, s, N=CH), 7.02 (2H, d, $J_{HH} = 7.2$ Hz, aryl *m*-H), 6.94 (1H, br s, pyrrole H4), 6.82 (1H, t, $J_{HH} = 7.8$ Hz, aryl *p*-H), 6.45 (1H, d, $^{3}J_{HH} = 3.2$ Hz, pyrrole H5), 6.04 (1H, d, $^{3}J_{HH} = 3.2$ Hz, pyrrole H3), 2.12 (6H, s, aryl *o*-CH_3). NMR [δ_C (100 MHz, CD_3CN)]: 159.6 (N=CH), 154.6 (aryl *ipso*-C), 139.4 (pyrrole C2), 136.4 (aryl *o*-C), 130.0 (aryl *p*-C), 128.6 (aryl *m*-C), 123.0 (pyrrole C4), 119.0 (pyrrole C5), 109.8 (pyrrole C3), 18.8 (aryl *o*-CH_3). NMR [δ_{Na} (105 MHz, CD_3CN)]: 4.31 (s, $\Delta\nu_{1/2} = 428$ Hz).

Data for 3. HRMS Found: *m/z* 235.12148 $[M + H]^+$. Calc. For $[C_{14}H_{16}N_2Na]^+$: 235.12112. NMR [δ_H (300 MHz, CD_3CN)]: 7.69 (1H, s, N=CH), 6.93 (1H, s, pyrrole H5), 6.83 (2H, s, aryl *m*-H), 6.43 (1H, dd, $^{4}J_{HH} = 1.2$ Hz and $^{3}J_{HH} = 3.0$ Hz, pyrrole H3), 6.04 (1H, dd, $^{4}J_{HH} = 1.5$ Hz and $^{3}J_{HH} = 3.0$ Hz, pyrrole H4), 2.22 (6H, s, mesityl *p*-CH_3), 2.07 (12H, s, mesityl *o*-CH_3). NMR [δ_C (75 MHz, CD_3CN)]: 158.8 (N=CH), 151.7 (aryl *ipso*-C), 149.6 (pyrrole C2), 138.0 (aryl *p*-C), 134.0 (pyrrole C5), 132.2 (pyrrole C4 or C3), 129.5 (aryl *o*-C), 129.3 (aryl *m*-C), 109.8 (pyrrole C4 or C3), 20.7 (aryl *p*-CH_3), 18.7 (*o*-CH_3). NMR [δ_{Na} (105 MHz, CD_3CN)]: 4.39 (s, $\Delta\nu_{1/2} = 529$ Hz).

Table 3 Crystal data and structure refinement for compounds **I**, **I_A**, **IV**, **1** and $\mathbf{D^{IV}}$

Compound	**I**	**I_A**	**IV**	**1**	$\mathbf{D^{IV}}$
Formula	$C_{11}H_{10}N_2$	$C_{11}H_{10}N_2$	$C_{17}H_{22}N_2$	$C_{22}H_{18}N_4Na_2$	$C_{42}H_{62}N_4Na_2O_2$
M	170.21	170.21	254.37	384.38	700.94
λ/Å	0.71073	0.71073	0.71073	0.71073	0.71073
T/K	150	150	150	150	150
Crystal system	Orthorhombic	Monoclinic	Monoclinic	Monoclinic	Monoclinic
Space group	*Pbca*	$P2_1/c$	$P2_1/n$	$P2_1/n$	$P2_1/n$
a/Å	9.4490 (14)	12.0440(14)	17.197(2)	10.1739(15)	11.704(6)
b/Å	18.186 (3)	18.727(2)	10.6030(11)	10.0052(14)	10.390(4)
c/Å	21.204 (3)	16.3890(18)	17.6180(19)	19.371(3)	17.231(7)
α (°)	90	90	90	90	90
β (°)	90	91.941(8)	108.648(6)	94.439(9)	95.563(16)
γ (°)	90	90	90	90	90
V/Å^3	3643.7 (9)	3694.4(7)	3043.8(6)	1965.9(5)	2085.5(16)
Z	16	16	8	4	2
ρ_c/g cm^{-3}	1.241	1.224	1.110	1.299	1.116
μ/mm^{-1}	0.076	0.074	0.065	0.117	0.086
θ_{max} (°)	28.12	25.12	27.75	26.80	25.14
Total data	82 598	6493	7137	4182	3703
Unique data	4443	3996	4421	2321	1758
R_{int}	0.071	0.116	0.066	0.086	0.157
$R\,[I > 3\sigma(I)]$	0.0402	0.0471	0.053	0.051	0.057
wR_2	0.104	0.114	0.147	0.122	0.154
Goodness of fit	1.018	1.001	1.054	0.949	0.978
ρ min, ρ max	–0.210	–0.198	–0.256	–0.306	–0.225
	0.195	0.214	0.416	0.253	0.247

Data for 4. HRMS Found: m/z 277.16756 [M + H]$^+$. Calc. For [$C_{17}H_{22}N_2Na$]$^+$: 277.16807. NMR [δ_H (400 MHz, CD_2Cl_2)]: 7.89 (1H, s, N=CH), 7.15–7.07 (4H, m, aryl *m*-, *p*-H and pyrrole H5), 6.70 (1H, d, $^3J_{HH}$ = 2.8 Hz, pyrrole H3), 6.30–6.29 (1H, m, pyrrole H4), 3.41 (3.3H, q, $^3J_{HH}$ = 7.2 Hz, ($CH_3CH_2)_2O$), 3.07 (2H, h, $^3J_{HH}$ = 6.8 Hz, $CH(CH_3)_2$), 1.14 (12H, d, $^3J_{HH}$ = 6.8 Hz, $CH(CH_3)_2$), 1.09 (5H, t, $^3J_{HH}$ = 7.2 Hz, ($CH_3CH_2)_2O$). NMR [δ_H (400 MHz, C_6D_6)]: 7.78 (1H, s, N=CH), 7.18–7.08 (3H, m, aryl *m*- and *p*-H), 6.48–6.41 (2H, m, pyrrole H5 and H3), 6.19 (1H, br s, pyrrole H4), 3.24 (1.2H, q, $^3J_{HH}$ = 7.2 Hz, ($CH_3CH_2)_2O$), 3.14 (2H, h, $^3J_{HH}$ = 6.8 Hz, $CH(CH_3)_2$), 1.16 (12H, d, $^3J_{HH}$ = 6.8 Hz, $CH(CH_3)_2$), 1.10 (1.8H, t, $^3J_{HH}$ = 7.2 Hz, ($CH_3CH_2)_2O$). NMR [δ_H (400 MHz, CD_3CN)]: 7.72 (1H, s, N=CH), 7.13–7.11 (2H, d, $^3J_{HH}$ = 7.6 Hz, aryl *m*-H), 7.02–6.98 (1H, t, $^3J_{HH}$ = 7.6 Hz, aryl *p*-H), 6.96 (1H, br s, pyrrole H5), 6.49 (1H, dd, $^4J_{HH}$ = 1.2 Hz and $^3J_{HH}$ = 3.2 Hz, pyrrole H3), 6.08 (1H, dd, $^4J_{HH}$ = 1.6 Hz and $^3J_{HH}$ = 3.2 Hz, pyrrole H4), 3.43 (1.5H, q, $^3J_{HH}$ = 7.0 Hz, ($CH_3CH_2)_2O$), 3.15 (2H, h, $^3J_{HH}$ = 6.8 Hz, $CH(CH_3)_2$), 1.15–1.12 (14H, m, $CH(CH_3)_2$ and ($CH_3CH_2)_2O$). NMR [δ_C (100 MHz, CD_2Cl_2)]: 160.5 (N=CH), 150.2 (aryl *o*-C), 140.0 (aryl *p*-C), 139.2 (aryl *ipso*-C), 135.4 (pyrrole C2), 124.2 (pyrrole C5), 123.4 (aryl *m*-C), 119.7 (pyrrole C3), 110.9 (pyrrole C4), 66.1 (($CH_3CH_2)_2O$), 28.2 ($CH(CH_3)_2$), 24.2 ($CH(CH_3)_2$), 15.3 (($CH_3CH_2)_2O$). NMR [δ_C (100 MHz, CD_3CN)]: 158.8 (N=CH), 152.3 (aryl *o*-C), 140.7 (aryl *p*-C), 138.3 (aryl *ipso*-C), 135.0 (pyrrole C2), 123.8 (pyrrole C5), 123.6 (aryl *m*-C), 118.7 (pyrrole C3), 109.9 (pyrrole C4), 66.2 (($CH_3CH_2)_2O$), 28.4 ($CH(CH_3)_2$), 24.0 ($CH(CH_3)_2$), 15.6 (($CH_3CH_2)_2O$). NMR [δ_{Na} (105 MHz, CD_3CN)]: 4.23 (s, $\Delta\nu_{1/2}$ = 400 Hz).

Data for 4*. HRMS Found: m/z 277.16756 [M + H]$^+$. Calc. For [$C_{17}H_{22}N_2Na$]$^+$: 277.16807. NMR [δ_H (400 MHz, CD_3CN)]: 7.72 (1H, s, N=CH), 7.12 (2H, d, $^3J_{HH}$ = 7.6 Hz, aryl *m*-H), 7.01 (1H, t, $^3J_{HH}$ = 7.6 Hz, aryl *p*-H), 6.97 (1H, m, pyrrole H5), 6.48 (1H, dd, $^4J_{HH}$ = 1.2 Hz and $^3J_{HH}$ = 3.2 Hz, pyrrole H3), 6.07 (1H, dd, $^4J_{HH}$ = 1.6 Hz and $^3J_{HH}$ = 3.2 Hz, pyrrole H4), 3.15 (2H, h, $^3J_{HH}$ = 6.8 Hz, $CH(CH_3)_2$), 1.13 (12H, d, $^3J_{HH}$ = 6.8 Hz, $CH(CH_3)_2$), ($CH_3CH_2)_2O$ resonances absent. NMR [δ_C (100 MHz, CD_3CN)]: 159.0 (N=CH), 152.4 (aryl *o*-C), 140.7 (aryl *p*-C), 138.5 (aryl *ipso*-C), 135.3 (pyrrole C2), 123.8 (pyrrole C5), 123.6 (aryl *m*-C), 118.7 (pyrrole C3), 109.9 (pyrrole C4), 28.4 ($CH(CH_3)_2$), 24.0 ($CH(CH_3)_2$), ($CH_3CH_2)_2O$ resonances absent. NMR [δ_{Na} (105 MHz, CD_3CN)]: 4.59 (s, $\Delta\nu_{1/2}$ = 550 Hz).

X-Ray experimental data

Crystallographic and experimental details of crystal structure determinations are listed in Table 3. The crystals of complexes **1** and $\mathbf{D^{IV}}$ were selected under an inert atmosphere, covered with polyfluoroether oil, and mounted on a nylon loop. Crystallographic data for compounds **I**, **I_A**, **IV**, **1** and $\mathbf{D^{IV}}$ were collected using graphite monochromated Mo-Kα radiation (λ = 0.71073 Å) on a Bruker AXS-KAPPA APEX II diffractometer equipped with an Oxford Cryosystem open-flow nitrogen cryostat, at 150 K. Cell parameters were retrieved using Bruker SMART software and refined using Bruker SAINT on all observed reflections. Absorption corrections were applied using SADABS.[43] Structure solution and refinement were performed using direct methods with the programs SIR97,[44] SIR2004[45] and SHELXL[46] both included in the package of programs WINGX-Version 1.70.01.[47] Except for the N*H* hydrogen atoms in compounds **I**, **I_A** and **IV**, all hydrogen atoms were inserted in idealised positions and allowed to refine riding on the parent carbon atom. Figures were generated using ORTEP3.[48] Data were deposited in CCDC under the deposit numbers 727070 for **I**, 727071 for **I_A**, 727072 for **IV**, 727073 for **1** and 727074 for $\mathbf{D^{IV}}$ (ESI†).

Computational details

All calculations were performed using the GAUSSIAN 03 software package,[49] and the PBE1PBE functional, without symmetry constraints. That functional uses a hybrid generalised gradient approximation (GGA), including 25% mixture of Hartree–Fock[50] exchange with DFT[26] exchange–correlation, given by Perdew, Burke and Ernzerhof functional (PBE),[51] and has proven to perform well in the description of non-covalent interactions.[52] A standard 6-31G(d,p) basis set[53] was used for geometry optimisations. The energy values reported were obtained through single point calculations on the geometries obtained at the PBE1PBE/6-31G(d,p) level with the same functional and a standard 6-311+G(d,p) basis set.[54]

Acknowledgements

We thank the Fundação para a Ciência e Tecnologia for financial support (Projects PPCDT/QUI/59025/2004 and PTDC/QUI/65474/2006), co-financed by European Funds for Regional Development (FEDER) and for fellowships (SFRH/BD/16807/2004 and SFRH/BPD/47853/2008) to C.S.B.G. and D.S., respectively, and the Portuguese NMR Network (IST-UTL Centre) for providing access to the NMR facility.

References

1 K. Mashima and H. Tsuguri, *J. Organomet. Chem.*, 2005, **690**, 4414, and references cited therein.
2 For reviews on post-metallocene polymerisation catalysts see for example: (*a*) S. D. Ittel, L. K. Johnson and M. Brookhart, *Chem. Rev.*, 2000, **100**, 1169; (*b*) G. J. P. Britovsek, V. C. Gibson and D. F. Wass, *Angew. Chem., Int. Ed.*, 1999, **38**, 428; (*c*) V. C. Gibson and S. K. Spitzmesser, *Chem. Rev.*, 2003, **103**, 283.
3 R. H. Holm, A. Chakravorty and L. J. Theriot, *Inorg. Chem.*, 1966, **5**, 625, and references cited therein.
4 V. C. Gibson, P. J. Maddox, C. Newton, C. Redshaw, G. A. Solan, A.J.P. White and D. J. Williams, *Chem. Commun.*, 1998, 1651.
5 V. C. Gibson, C. Newton, C. Redshaw, G. A. Solan, A. J. P. White and D. J. Williams, *J. Chem. Soc., Dalton Trans.*, 2002, 4017.
6 (*a*) S. A. Carabineiro, L. C. Silva, P. T. Gomes, L. C. J. Pereira, L. F. Veiros, S. I. Pascu, M. T. Duarte, S. Namorado and R. T. Henriques, *Inorg. Chem.*, 2007, **46**, 6880; (*b*) S. A. Carabineiro, P. T. Gomes, L. F. Veiros, C. Freire, L. C. J. Pereira, R. T. Henriques, J. E. Warren and S. I. Pascu, *Dalton Trans.*, 2007, 5460; (*c*) S. A. Carabineiro, R. M. Bellabarba, P. T. Gomes, S. I. Pascu, L. F. Veiros, C. Freire, L. C. J. Pereira, R. T. Henriques, M. C. Oliveira and J. E. Warren, *Inorg. Chem.*, 2008, **47**, 8896.
7 D. M. Dawson, D. A. Walker, M. Thornton-Pett and M. Bochmann, *J. Chem. Soc., Dalton Trans.*, 2000, 459.
8 R. M. Bellabarba, P. T. Gomes and S. I. Pascu, *Dalton Trans.*, 2003, 4431.
9 P. Pérez-Puente, E. de Jésus, J. C. Flores and P. Gómez-Sal, *J. Organomet. Chem.*, 2008, **693**, 3902.
10 H. Hao, S. Bhandari, Y. Ding, H. W. Roesky, J. Magull, H. G. Schmidt, M. Noltemeyer and C. Cui, *Eur. J. Inorg. Chem.*, 2002, 1060.
11 C. S. B. Gomes, P. T. Gomes, R. E. Di Paolo, A. L. Maçanita, M. T. Duarte and M. J. Calhorda, *Inorg. Chem.*, 2009, DOI: 10.1021/ic901519s, in press.
12 Y. Matsuo, K. Mashima and K. Tani, *Chem. Lett.*, 2000, 1114.
13 Y. Yoshida, S. Matsiu, Y. Takagi, M. Mitani, M. Nitabaru, T. Nakano, H. Tanaka and T. Fujita, *Chem. Lett.*, 2000, 1270.
14 Y. Yoshida, S. Matsiu, Y. Takagi, M. Mitani, T. Nakano, H. Tanaka, N. Kashiwa and T. Fujita, *Organometallics*, 2001, **20**, 4793.
15 Y. Yoshida, J. Saito, M. Mitani, Y. Takagi, S. Matsui, S. Ishii, T. Nakano, N. Kashiwa and T. Fujita, *Chem. Commun.*, 2002, 1298.
16 Y. Yoshida, J. Mohri, S. Ishii, M. Mitani, J. Saito, S. Matsui, H. Makio, T. Nakano, H. Tanaka, M. Onda, Y. Yamamoto, A. Mizuno and T. Fujita, *J. Am. Chem. Soc.*, 2004, **126**, 12023.
17 S. Matsui, T. P. Spaniol, Y. Tagaki, Y. Yoshida and J. Okuda, *J. Chem. Soc., Dalton Trans.*, 2002, 4529.
18 S. Matsui, Y. Yoshida, Y. Tagaki, T. P. Spaniol and J. Okuda, *J. Organomet. Chem.*, 2004, **689**, 1155.
19 Y. Matsuo, K. Mashima and K. Tani, *Organometallics*, 2001, **20**, 3510.
20 C. Cui, A. Shafir, C. L. Reeder and J. Arnold, *Organometallics*, 2003, **22**, 3357.
21 For example: (*a*) A. Efraty, N. Jubran and A. Goldman, *Inorg. Chem.*, 1982, **21**, 868; (*b*) N. Kuhn, *Bull. Soc. Chim. Belg.*, 1990, **99**, 707; (*c*) A. Novak, A. J. Blake, C. Wilson and J. B. Love, *Chem. Commun.*, 2002, 2796; (*d*) N. I. Pyshnograeva, V. N. Setkina, A. S. Batsanov and Yu. T. Struchkov, *J. Organomet. Chem.*, 1985, **288**, 189; (*e*) G. Gao, I. Korobkov and S. Gambarotta, *Inorg. Chem.*, 2004, **43**, 1108; (*f*) J. B. Love, A. J. Blake, C. Wilson, S. D. Reid, A. Novak and P. B. Hitchcock, *Chem. Commun.*, 2003, 1682; (*g*) S. D. Reid, A. J. Blake, C. Wilson and J. B. Love, *Inorg. Chem.*, 2006, **45**, 636; (*h*) A. Athimoolam, S. Gambarotta and I. Korobkov, *Can. J. Chem.*, 2005, **83**, 832; (*i*) A. M. Galvão, *PhD*, *Thesis*, Instituto Superior Técnico, Lisboa, 1999, and references cited therein.
22 (*a*) M. Ganesan, C. D. Bérubé, S. Gambarotta and G. P. A. Yap, *Organometallics*, 2002, **21**, 1707; (*b*) T. Dube, D. Freckmann, S. Conoci, S. Gambarotta and G. P. A. Yap, *Organometallics*, 2000, **19**, 209; (*c*) G. Aharonian, S. Gambarotta and G. P. A. Yap, *Organometallics*, 2002, **21**, 4257.
23 (*a*) D. Jacoby, C. Floriani, A. Chiesi-Villa and C. Rizzoli, *J. Am. Chem. Soc.*, 1993, **115**, 3595; (*b*) E. Campazzi, E. Solari, R. Scopelliti and C. Floriani, *Chem. Commun.*, 1999, 1617; (*c*) L. Bonomo, C. Stern, E. Solari, R. Scopelliti and C. Floriani, *Angew. Chem., Int. Ed.*, 2001, **40**, 1449; (*d*) J. Bachmann and D. G. Nocera, *J. Am. Chem. Soc.*, 2005, **127**, 4730.
24 N. Kuhn, G. Henkel and J. Kreutzberg, *Angew. Chem., Int. Ed. Engl.*, 1990, **29**, 1143.
25 R. E. Mulvey, *Chem. Soc. Rev.*, 1991, **20**, 167, and references cited therein.
26 R. G. Parr and W. Yang, *Density Functional Theory of Atoms and Molecules*, Oxford University Press, New York, 1989.
27 The crystal data of polymorph **I_A** is contained in the joint cif file available in the ESI. †Fig. S1 and Table S1 of the ESI show the asymmetric unit of **I_A** and the corresponding selected bond distances and angles, respectively.
28 O. Q. Munro, S. D. Joubert and C. D. Grimmer, *Chem.–Eur. J.*, 2006, **12**, 7987.
29 (*a*) S. Beaini, G. B. Deacon, A. P. Erven, P. C. Junk and D. R. Turner, *Chem.–Asian J.*, 2007, **2**, 539; (*b*) S.-A. Cortés-Llamas, R. Hernández-Lamoneda, M.-A. Velázquez-Carmona, M.-A. Muñoz-Hernández and R. A. Toscano, *Inorg. Chem.*, 2006, **45**, 286.
30 (*a*) M. Nishio, *CrystEngComm*, 2004, **6**, 130; (*b*) M. Nishio, Y. Umezawa, K. Honda, S. Tsuboyama and H. Suezawa, *CrystEngComm*, 2009, **11**, 1757.
31 R. Hacker, E. Kaufmann, P. von R. Schleyer, W. Mahdi and H. Dietrich, *Chem. Ber.*, 1987, **120**, 1533.
32 (*a*) In fact, ^{23}Na NMR is not a widely used technique, and a typical scale for the variation of ^{23}Na chemical shifts is much more complex and of much less straightforward structural interpretation than those of ^{1}H or ^{13}C NMR. However, as reference values, we may provide examples such as the ^{23}Na chemical shift of a $NaClO_4$ in acetonitrile-d_6, which is −6.35 ppm ($\Delta\nu_{1/2} = 7$ Hz)[32b] or, the spread in ^{23}Na chemical shifts of 22 ppm (−11 to +11 ppm) observed in a series of three sodium cryptands with 4 to 6 coordinating O atoms[32c]; (*b*) M. Beltowska-Brzezinska, T. Luczak, B. Gierczyk, K. Eitner, B. Brzezinski, R. Pankiewicz and G. Schroeder, *J. Mol. Struct.*, 2002, **607**, 77; (*c*) P. Laszlo, *Angew. Chem., Int. Ed.*, 1978, **17**, 254, and references cited therein.
33 J. W. Akitt and W. S. McDonald, *J. Magn. Reson.*, 1984, **58**, 401.
34 A. Wong and G. Wu, *J. Phys. Chem. A*, 2000, **104**, 11844, and references therein.
35 C. M. Widdifield, J. A. Tang, C. L. B. MacDonald and R. W. Schurko, *Magn. Reson. Chem.*, 2007, **45**, S116.
36 M. J. Willians and R. W. Schurko, *J. Phys. Chem. B*, 2003, **107**, 5144.
37 See for instance:H. Saitô and R. Tabeta, *Bull. Chem. Soc. Jpn.*, 1987, **60**, 61.
38 J. P. Amoureux, C. Fernandez, L. Carpentier and E. Cochon, *Phys. Status Solidi A*, 1992, **132**, 461.

39 D. O. A. Garrido, G. Buldain and B. Frydman, *J. Org. Chem.*, 1984, **49**, 2619.
40 K.-N. Yeh and R. H. Barker, *Inorg. Chem.*, 1967, **6**, 830.
41 (*a*) Y.-S. Li, Y.-R. Li and X.-F. Li, *J. Organomet. Chem.*, 2003, **667**, 185; (*b*) D. M. Antonelli, P. T. Gomes, M. L. H. Green, A. M. Martins and P. Mountford, *J. Chem. Soc., Dalton Trans.*, 1997, 2435; (*c*) M. Jiménez-Tenorio, M. C. Puerta, I. Salcedo, P. Valerga, S. I. Costa, P. T. Gomes and K. Mereiter, *Chem. Commun.*, 2003, 1168; (*d*) H.-R. Liu, S. I. Costa, P. T. Gomes, M. T. Duarte, R. Branquinho, A. C. Fernandes, J. C. W. Chien and M. M. Marques, *J. Organomet. Chem.*, 2005, **690**, 1314.
42 C. N. Iverson, C. A. S. G. Carter, R. T. Baker, J. D. Scollard, J. A. Labinger and J. E. Bercaw, *J. Am. Chem. Soc.*, 2003, **125**, 12674.
43 G. M. Sheldrick, *SADABS, Program for Empirical Absorption Correction*, University of Göttingen, Göttingen, Germany, 1996.
44 SIR97 -A. Altomare, M. C. Burla, M. Camalli, G. L. Cascarano, C. Giacovazzo, A. Guagliardi, A. G. G. Moliterni, G. Polidori and R. Spagna, *J. Appl. Crystallogr.*, 1999, **32**, 115.
45 SIR2004 -M. C. Burla, R. Caliandro, M. Camalli, B. Carrozzini, G. L. Cascarano, L. De Caro, C. Giacovazzo, G. Polidori and R. Spagna, *J. Appl. Crystallogr.*, 2005, **38**, 381.
46 (*a*) G. M. Sheldrick, *SHELX97 - Programs for Crystal Structure Analysis (Release 97-2)*, Institüt für Anorganische Chemie der Universität, Tammanstrasse 4, D-3400 Göttingen, Germany, 1998; (*b*) G. M. Sheldrick, *Acta Crystallogr., Sect. A: Found. Crystallogr.*, 2008, **64**, 112.
47 L. J. Farrugia, *J. Appl. Crystallogr.*, 1999, **32**, 837.
48 ORTEP3 for Windows -L. J. Farrugia, *J. Appl. Crystallogr.*, 1997, **30**, 565.
49 M. J. Frisch, G. W. Trucks, H. B. Schlegel, G. E. Scuseria, M. A. Robb, J. R. Cheeseman, J. A. Montgomery, Jr., T. Vreven, K. N. Kudin, J. C. Burant, J. M. Millam, S. S. Iyengar, J. Tomasi, V. Barone, B. Mennucci, M. Cossi, G. Scalmani, N. Rega, G. A. Petersson, H. Nakatsuji, M. Hada, M. Ehara, K. Toyota, R. Fukuda, J. Hasegawa, M. Ishida, T. Nakajima, Y. Honda, O. Kitao, H. Nakai, M. Klene, X. Li, J. E. Knox, H. P. Hratchian, J. B. Cross, C. Adamo, J. Jaramillo, R. Gomperts, R. E. Stratmann, O. Yazyev, A. J. Austin, R. Cammi, C. Pomelli, J. W. Ochterski, P. Y. Ayala, K. Morokuma, G. A. Voth, P. Salvador, J. J. Dannenberg, V. G. Zakrzewski, S. Dapprich, A. D. Daniels, M. C. Strain, O. Farkas, D. K. Malick, A. D. Rabuck, K. Raghavachari, J. B. Foresman, J. V. Ortiz, Q. Cui, A. G. Baboul, S. Clifford, J. Cioslowski, B. B. Stefanov, G. Liu, A. Liashenko, P. Piskorz, I. Komaromi, R. L. Martin, D. J. Fox, T. Keith, M. A. Al-Laham, C. Y. Peng, A. Nanayakkara, M. Challacombe, P. M. W. Gill, B. Johnson, W. Chen, M. W. Wong, C. Gonzalez, and J. A. Pople, *Gaussian 03, Revision C.02*, Gaussian Inc., Wallingford CT, 2004.
50 W. J. Hehre, L. Radom, P. v. R. Schleyer, J. A. Pople, *Ab Initio Molecular Orbital Theory*, John Wiley & Sons, New York, 1986.
51 (*a*) J. P. Perdew, K. Burke and M. Ernzerhof, *Phys. Rev. Lett.*, 1997, **78**, 1396; (*b*) J. P. Perdew, *Phys. Rev. B: Condens. Matter Mater. Phys.*, 1986, **33**, 8822.
52 Y. Zhao and D. G. Truhlar, *J. Chem. Theory Comput.*, 2005, **1**, 415.
53 (*a*) R. Ditchfield, W. J. Hehre and J. A. Pople, *J. Chem. Phys.*, 1971, **54**, 724; (*b*) W. J. Hehre, R. Ditchfield and J. A. Pople, *J. Chem. Phys.*, 1972, **56**, 2257; (*c*) P. C. Hariharan and J. A. Pople, *Mol. Phys.*, 1974, **27**, 209; (*d*) M. S. Gordon, *Chem. Phys. Lett.*, 1980, **76**, 163; (*e*) P. C. Hariharan and J. A. Pople, *Theor. Chim. Acta*, 1973, **28**, 213.
54 (*a*) A. D. McClean and G. S. Chandler, *J. Chem. Phys.*, 1980, **72**, 5639; (*b*) R. Krishnan, J. S. Binkley, R. Seeger and J. A. Pople, *J. Chem. Phys.*, 1980, **72**, 650; (*c*) A. J. H. Wachters, *J. Chem. Phys.*, 1970, **52**, 1033; (*d*) P. J. Hay, *J. Chem. Phys.*, 1977, **66**, 4377; (*e*) K. Raghavachari and G. W. Trucks, *J. Chem. Phys.*, 1989, **91**, 1062; (*f*) R. C. Binning and L. A. Curtiss, *J. Comput. Chem.*, 1990, **11**, 1206; (*g*) M. P. McGrath and L. Radom, *J. Chem. Phys.*, 1991, **94**, 511.

